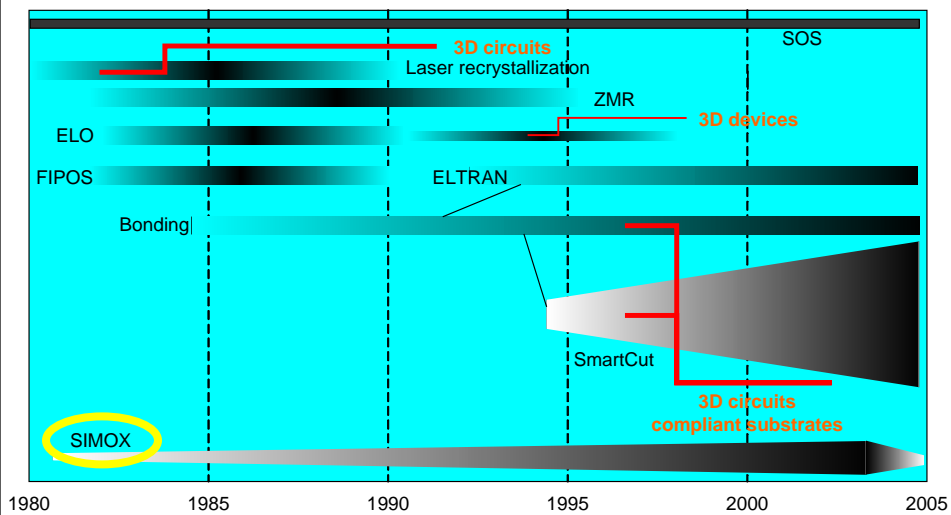


Modern SOI Materials

Jean-Pierre Colinge
University of California, Davis

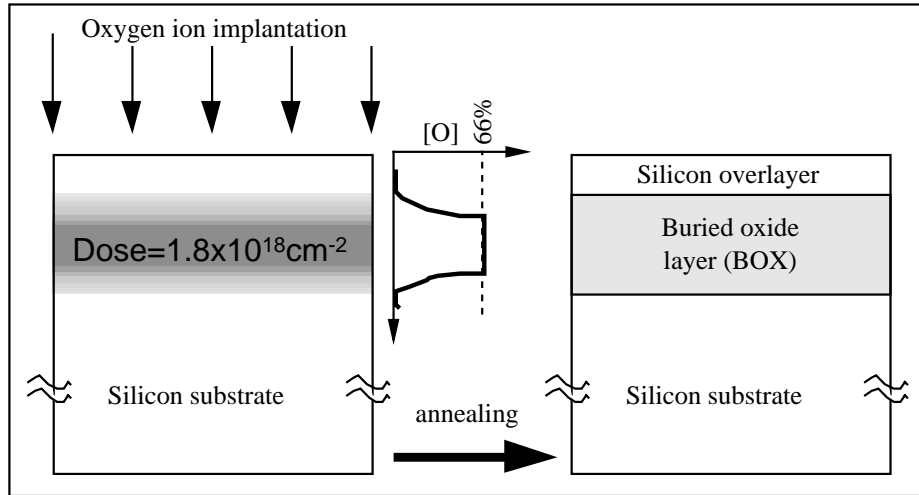
1

SOI Materials



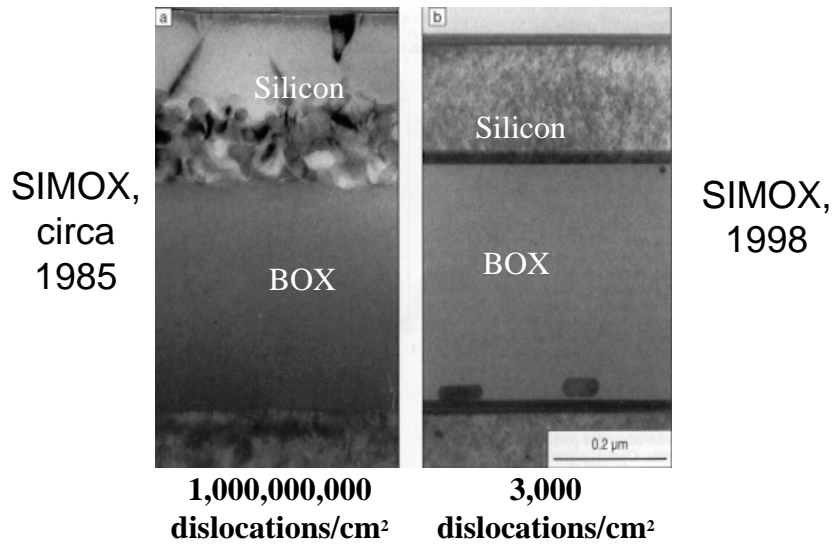
2

Principle of SIMOX



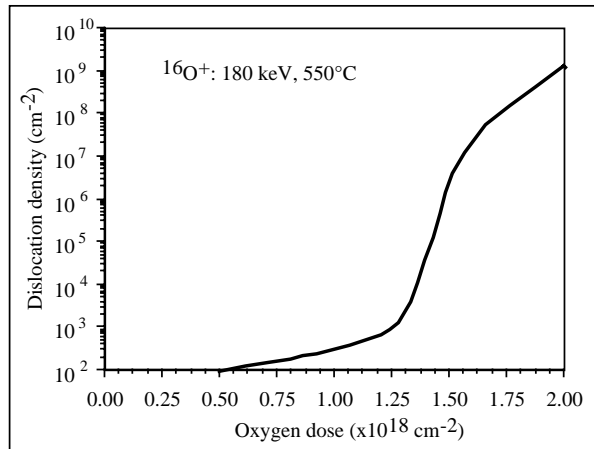
3

Evolution of SIMOX quality



4

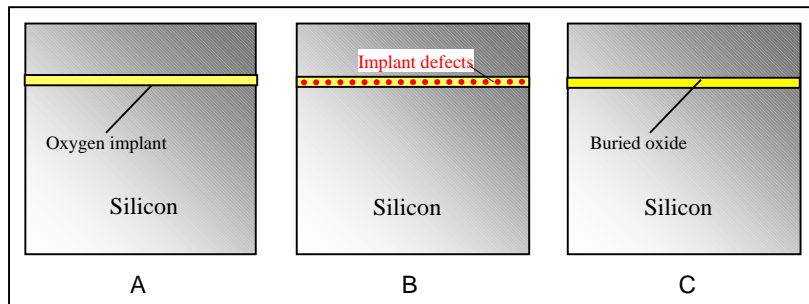
Modified low-dose SIMOX (SIMOX-MLD)



Evolution of dislocation density in the silicon overlayer with implanted oxygen dose

5

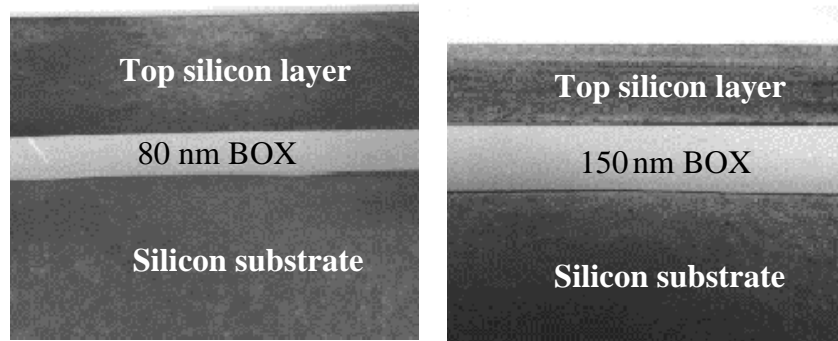
Modified low-dose SIMOX (SIMOX-MLD)



A: First implant $3 \times 10^{17} \text{ O}^+ \text{ cm}^{-2}$, 120 keV, 525°C
B: Second implant $10^{15} \text{ O}^+ \text{ cm}^{-2}$, >120 keV, room Temp.
C: Final annealing

6

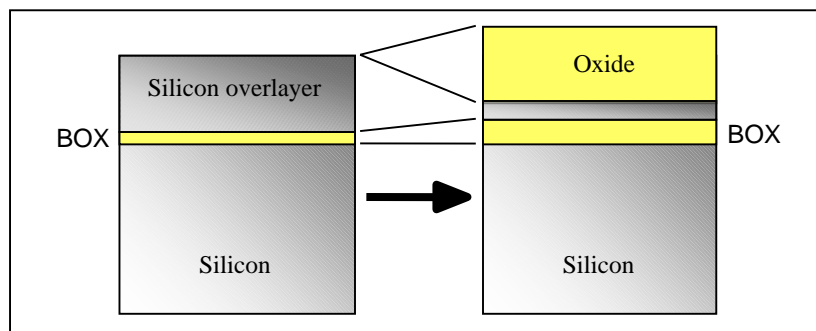
Modified low-dose SIMOX (SIMOX-MLD)



Typical MLD: Dose= $3 \times 10^{17} \text{cm}^{-2} + 10^{15} \text{cm}^{-2}$

7

Variations on the SIMOX theme: ITOX



Principle of internal thermal oxidation (ITOX)

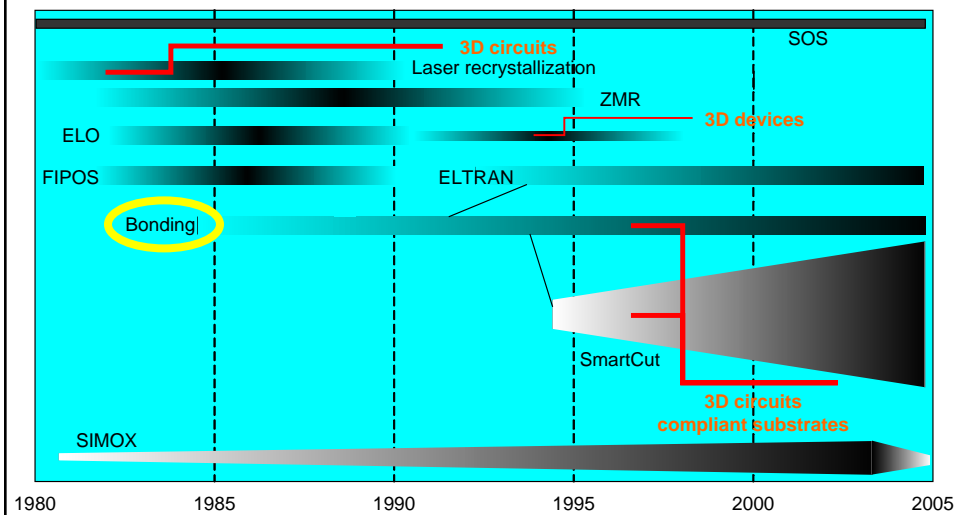
8

SIMOX material properties

Parameter	Standard SIMOX	SIMOX MLD
Wafer diameter	up to 200 mm	up to 300 mm
Silicon film thickness	210 nm	20 to 145 nm
Silicon film thickness uniformity		±2 nm
Buried oxide (BOX) thickness	375 nm	135, 145 nm
Buried oxide (BOX) thickness uniformity	±10 nm	±5 nm
Surface roughness (RMS)	0.7 nm	<0.15 nm
Dislocation density	< 1000 cm ⁻²	< 1000 cm ⁻²
HF defect density	< 0.5 cm ⁻²	< 0.1 cm ⁻²
BOX pipe (pinhole) density	< 0.1 cm ⁻²	< 0.1 cm ⁻²
Metallic contamination	< 5x10 ¹⁰ cm ⁻²	< 3x10 ¹⁰ cm ⁻²
BOX dielectric breakdown	>5 MV/cm	>7 MV/cm

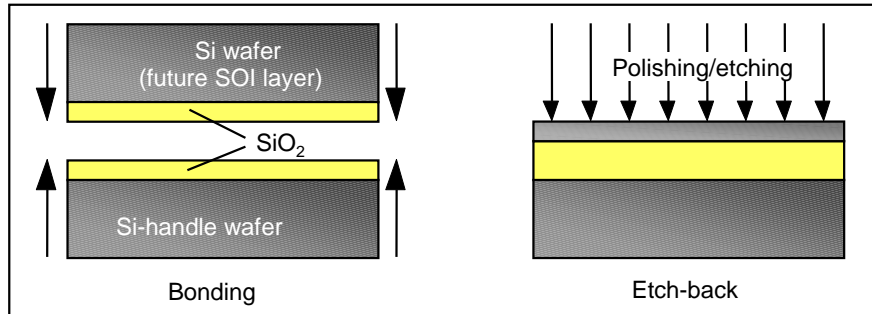
9

SOI Materials



10

Bonded and Etch-back SOI (BESOI)



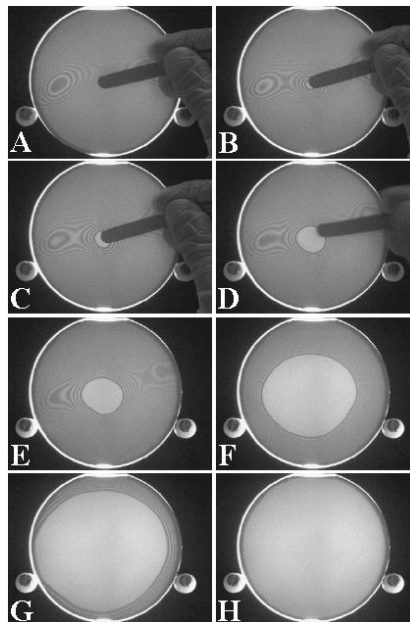
Bonding of two oxidized silicon wafers (left) and polishing/etching back of one of the wafers

11

Bonding mechanism

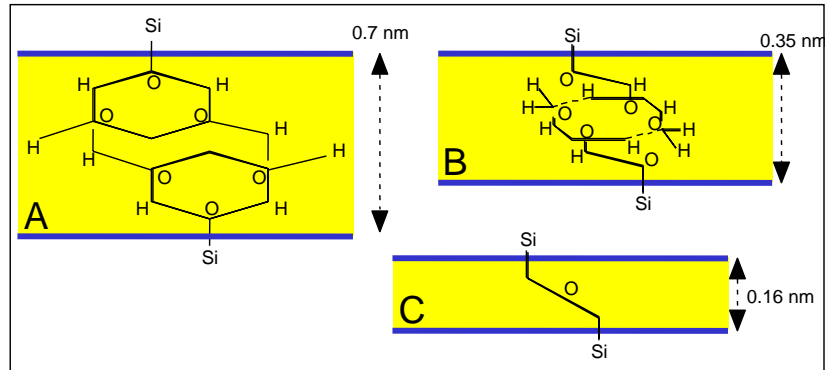
Infrared transmission imaging showing the propagation of a bonding wave between two oxidized 100-mm silicon wafers (from A to H). Time between different pictures is approximately 0.5 second.

Movie can be viewed at:
<http://www.waferbond.com/>



12

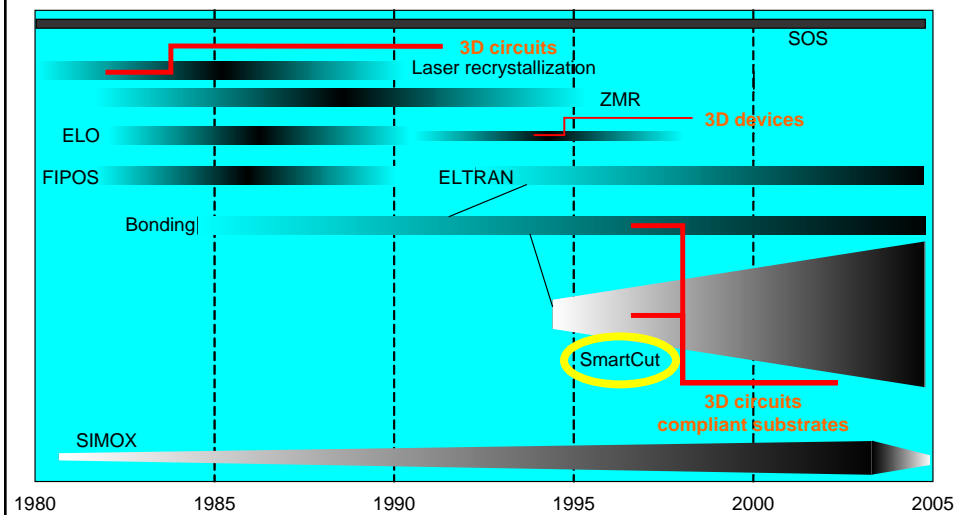
Stengl's model for silicon wafer bonding



A: Room temperature, $\text{SiOH}:(\text{OH}_2)_2:(\text{OH}_2)_2:\text{HOSi}$;
 B: $T = 200^\circ\text{C}$, $\text{SiOH}:\text{HOSi} + (\text{H}_2\text{O})_4$
 C: $T > 700^\circ\text{C}$, $\text{SiOSi} + \text{H}_2\text{O}$

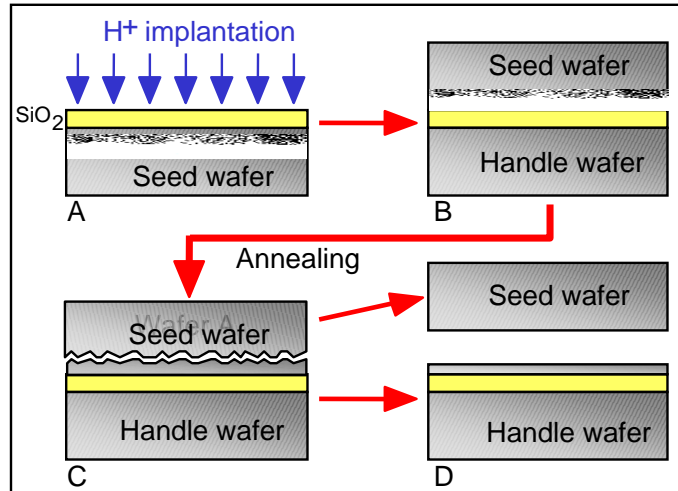
13

SOI Materials



14

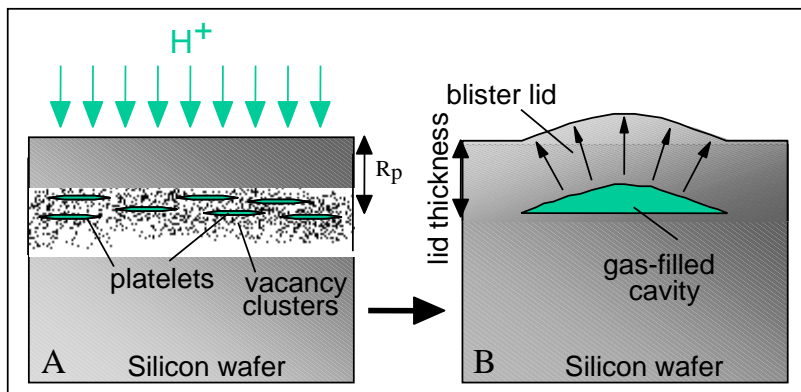
Smart-Cut[®] process



A: Hydrogen implantation; B: Wafer bonding; C: Splitting of wafer A; D: Polishing of both wafers. Wafer A is recycled as a future handle wafer

15

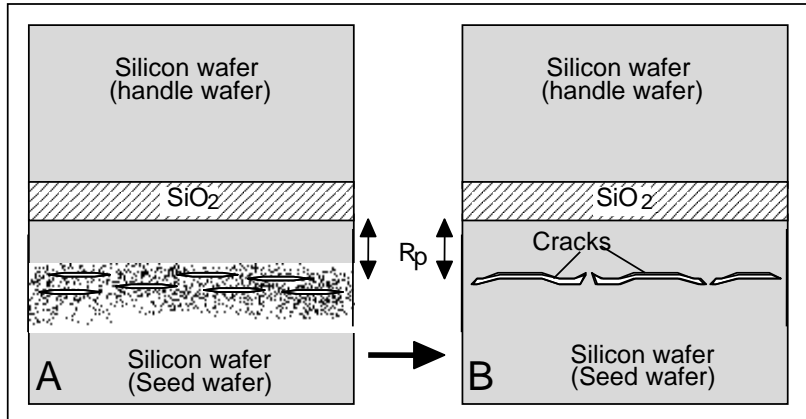
Smart-Cut[®] process



A: Hydrogen implantation and formation of defects (vacancies, vacancy clusters and platelets); B: Formation of a blister upon annealing. R_p is the projected range of the implanted ions.

16

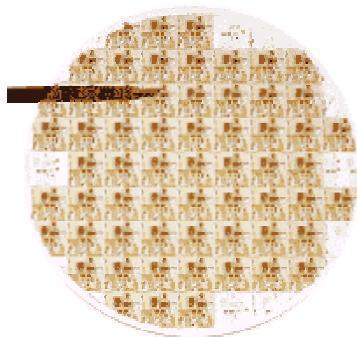
Smart-Cut[®] process



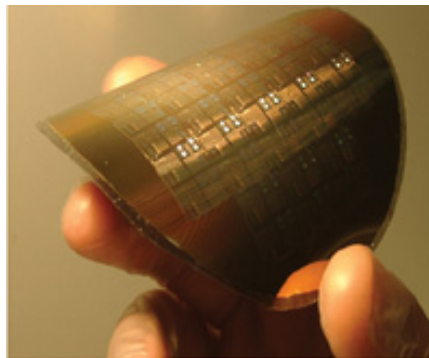
Formation of cracks near the projected range of a silicon wafer implanted with hydrogen. A: Bonding of the handle wafer (stiffener) to the seed wafer; B: Formation of a crack network near the projected range upon annealing.

17

Layer transfer using bonding Techniques



SOI devices transferred onto 200 mm fused silica wafer

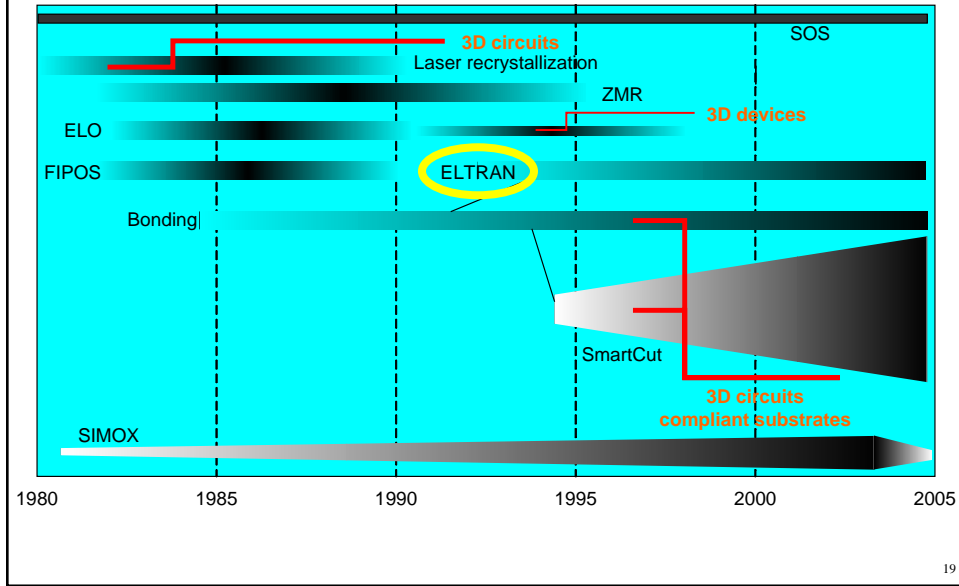


Bulk devices thinned down to 35 μm and transferred onto a plastic film

<http://www.tracit-tech.com/transfer.html>

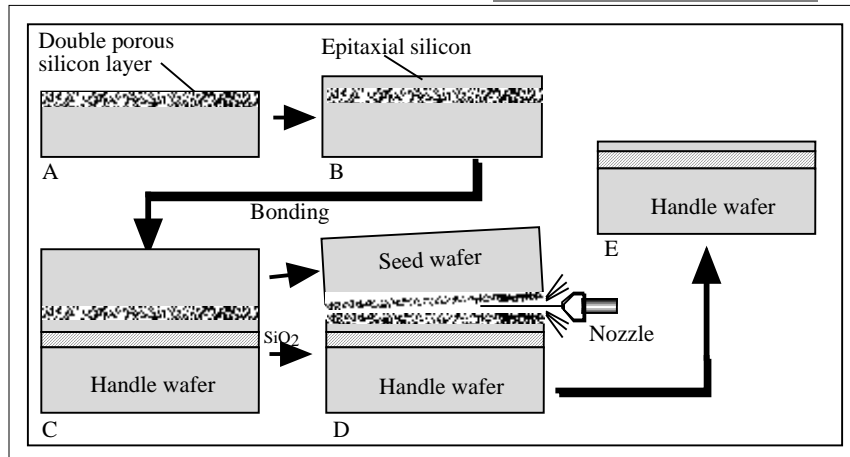
18

SOI Materials



19

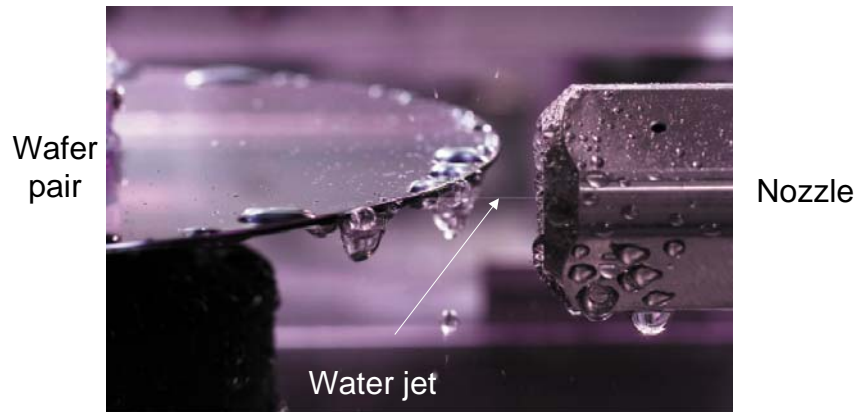
Eltran® process



A: Formation of a porous silicon layer by electrochemical reaction in HF;
 B: Growth of epitaxial silicon; C: Bonding to a handle wafer; D: Porous silicon layer splitting using a water jet; E: Etching and H₂ annealing.

20

Eltran® process



<http://www.canon.com/technology/detail/device/soi/>

http://www.mrs.org/meetings/spring2001/presentations/SO118.2_color.pdf

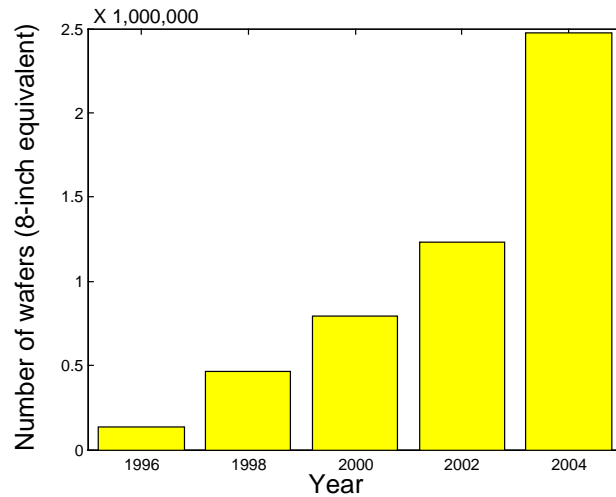
21

Transferred layer material properties

Parameter	Unibond®	Eltran®
Wafer diameter	300 mm	300 mm
Silicon film thickness	50 to 100 nm	20 to 145nm
Silicon film thickness uniformity	± 0.5 nm	±1.6 nm
Buried oxide (BOX) thickness	100 nm to 3 μm	135, 145 nm
Buried oxide thickness uniformity	±0.1 nm	±2 nm
Surface roughness (RMS)	0.15 nm	0.1 nm
Dislocation density	100 cm ⁻²	400 cm ⁻²
HF defect density	1 cm ⁻²	< 0.05 cm ⁻²
BOX pipe (pinhole) density	none	none
Metallic contamination	5x10 ¹⁰ cm ⁻²	5x10 ¹⁰ cm ⁻²

22

Estimated worldwide SOI wafer production capability



23

SOI CMOS Processing and Design Issues

Jean-Pierre Colinge
University of California, Davis

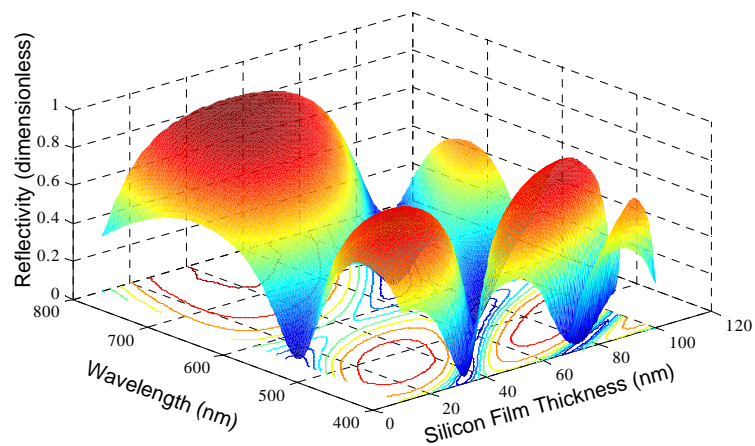
24

Outline

- Evaluation of SOI wafers
- Process-related metrology issues
- SOI vs. bulk CMOS processing
- Process steps and processing issues specific to SOI

25

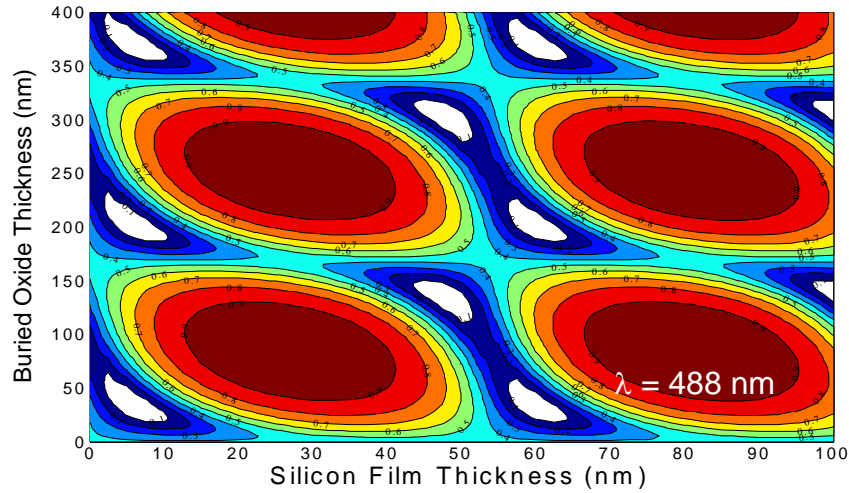
Thickness measurement/Reflectometry



Reflectivity of the SOI structure as a function of wavelength and silicon film thickness. The BOX thickness is 400 nm.

26

Metrology issue: haze/particulate detection



Apparent particulate size depends on reflectivity !

C. Maleville, E. Neyret, L. Ecarnot, T. Barge, A.J. Auberton, Proceedings of the IEEE International SOI Conference, p. 19, 2001
 C. Maleville, Electrochemical Society Proceedings Vol. 2003-05, p. 33, 2003
 C. Maleville, C. Moulin, E. Neyret, Proceedings of the IEEE International SOI Conference, p. 194, 2002

27

Chemical decoration of defects

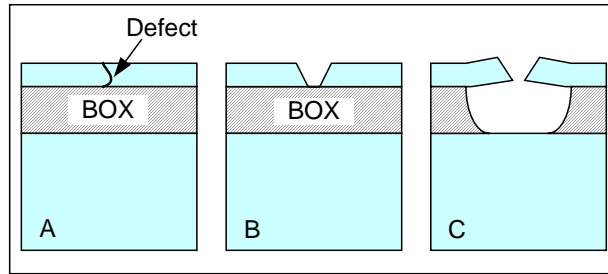
Dash etch	HF:HNO ₃ :CH ₃ COOH 1:3:10
Schimmel etch	HF:1M CrO ₃ 2:1
Secco etch	HF:0.15M K ₂ Cr ₂ O ₇ 2:1
Stirl etch	HF:5M CrO ₃ 1:1
Wright etch	60ml HF:30 ml HNO ₃ :30 ml 5M CrO ₃ : 2 grams Cu(NO ₃) ₂ :60 ml H ₂ O
Electrochemical etch	5% wt HF
Iodine etch	2M KI:0.5M I ₂ :2.5M HF:28.5M CH ₃ OH:66.5M H ₂ O

W.C. Dash, J. Appl. Phys. Vol. 27, p. 1993, 1956
 D.G. Schimmel, J. Electrochem. Soc. Vol. 126, p. 479, 1979
 F. Secco d'Aragona, J. Electrochem. Soc., Vol. 119, p. 948, 1972
 E. Sirtl and A. Adler, Zeitung für Metallkunde, Vol. 52, p. 529, 1961
 M. Wright Jenkins, J. Electrochem. Soc., Vol. 124, p. 757, 1977
 T.R. Guilinger, M.J. Kelly, J.W. Medernach, S.S. Tsao, J.O. Steveson, and H.D.T. Jones, Proceedings of the IEEE SOS/SOI Technology Conference, p. 93, 1989
 M.J. Kelly, T.R. Guilinger, J.W. Medernach, S.S. Tsao, H.D.T. Jones, and J.O. Steveson, Electrochemical Society Proceedings, Vol. 90-6, p. 120, 1990
 K. Inamura, K. Daido, K. Mimegishi, H. Nakanishi, Japanese Journal of Applied Physics, Vol.16, suppl.1, p. 547, 1977
 Y. Moriyasu, T. Morishita, M. Matsui, A. Yasujima, M. Ishida, Electrochemical Society Proceedings, Vol. 99-3, p. 137, 1999

28

Chemical decoration of defects

Problem: Si film may be too thin and is etched before defects are decorated.

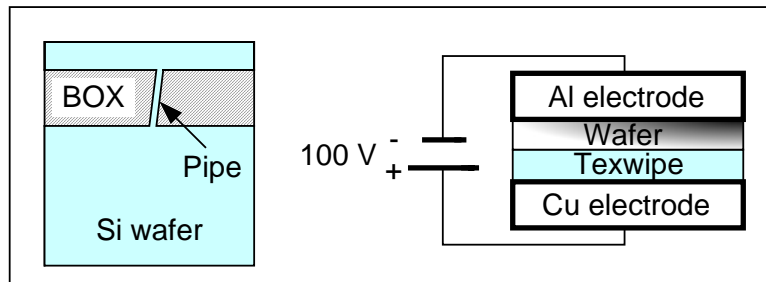


Defect in thin SOI layer (A) revealed by Secco etch (B) followed by HF etch (C)

H. Moriceau, B. Aspar, M. Bruel, A.M. Cartier, C. Morales, A. Soubie, T. Barge, S. Bressot, C. Maleville, A.J. Auberton, Electrochemical Society Proceedings, Vol. 99-3, p. 173, 1999

29

Chemical decoration of BOX pipes

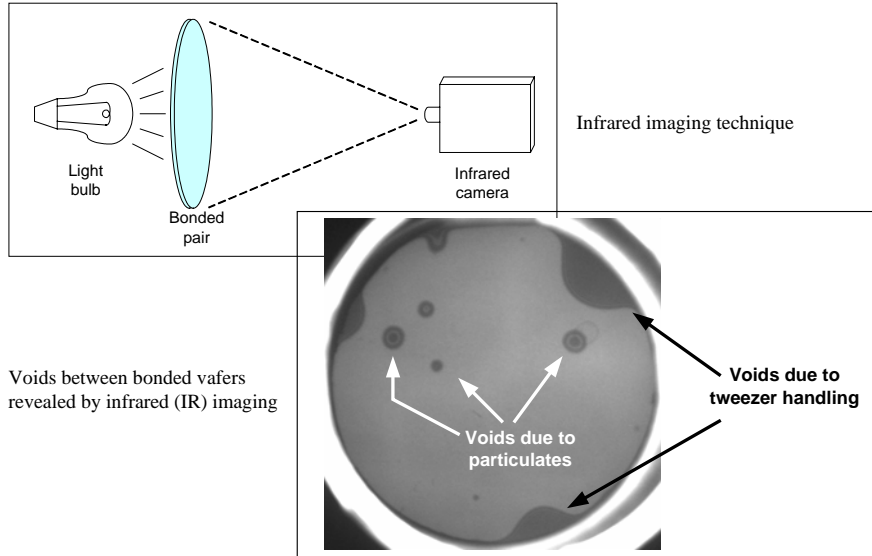


The electrolytic reaction $CuSO_4 \rightarrow Cu^{++} + SO_4^-$ and $Cu^{++} + 2e^- \rightarrow Cu(s)$ takes place in the Texwipe™ wherever it receives current from a pipe. Stains (dots) of metallic copper are, therefore, created on the Texwipe™, each corresponding to a pipe in the BOX

L.P. Allen, M.J. Anc, M. Duffy, J.H. Parechian, J.H. Yap, Electrochemical Society Proceedings Vol. 96-3, p. 18, 1996

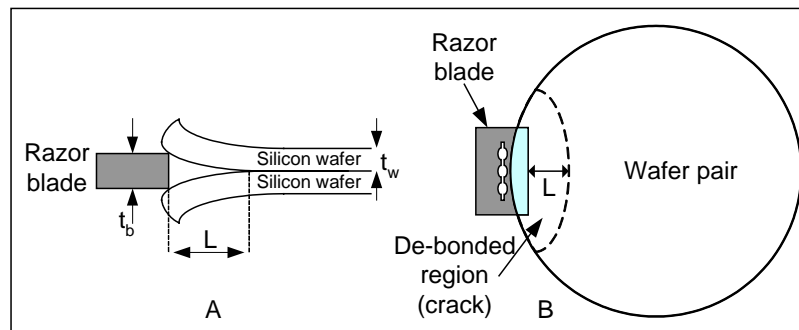
30

Wafer Bonding Quality



31

Bonding Strength



Crack propagation measurement; A: lateral view; B: top view

The strength of the bond (or bonding energy) is measured in erg/cm^2 or J/m^2 ($1 \text{ erg}/\text{cm}^2 = 10^{-3} \text{ J}/\text{m}^2$). The most common technique used to measure bond energy is the so-called "crack propagation technique" based on the insertion of a razor blade between the bonded wafers (Figure 3.12). The insertion of a blade of thickness t_b causes the formation of a "crack" or a de-bonded region that extends over a length L past the edge of the blade. The extension of the crack can be measured by infrared imaging. The bond energy, γ , is given by:

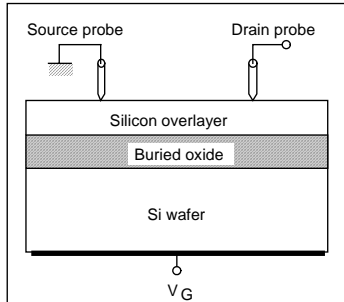
$$\gamma = \frac{3Et_w^3 t_b^2}{32 L^4} \quad (\text{J}/\text{m}^2)$$

where t_w is the thickness of each individual wafer (m), E is the silicon Young's modulus (166 GPa) and L is the crack length (m). This measurement is very easy to perform, but any inaccuracy in measuring the crack length induces large variations of the calculated bonding energy, because of the fourth-power dependence of γ on L . A 10% inaccuracy in crack length measurement, for instance, leads to a near 50% error in bonding energy.

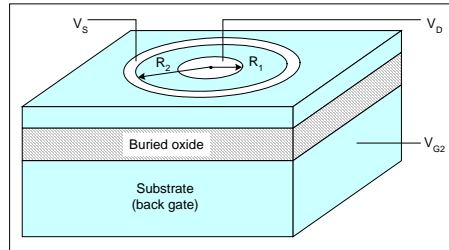
W.P. Maszarn, G. Goetz, A. Caviglia, J.B. McKitterick, *Journal of Applied Physics*, Vol. 64, p. 4943, 1988
 Q.Y. Tong and U. Gösele, *Semiconductor Wafer Bonding Science and Technology*, The Electrochemical Society Series, John Wiley & Sons, p. 25, 1999

32

Ψ-MOSFET



Principle of the Ψ-MOSFET



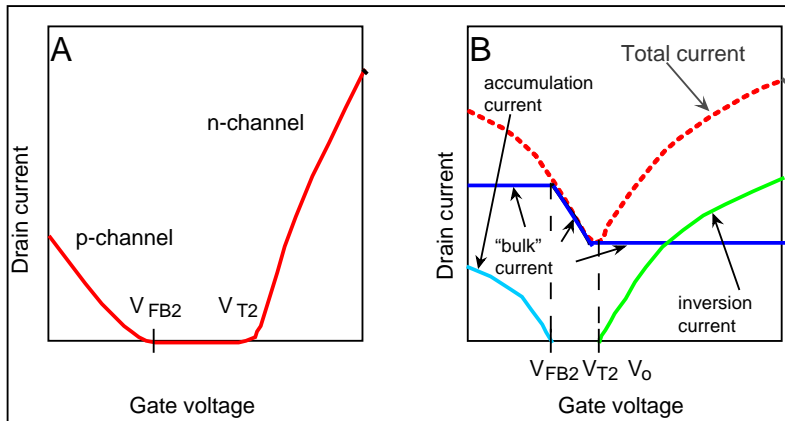
Ψ-MOSFET with circular, concentric source and drain electrodes

$$I_D = f_g C_{ox2} \frac{H_0}{1 + \theta(V_{G2} - V_{T2/FB2})} (V_{G2} - V_{T2/FB2}) V_D$$

$$I_D = \frac{2\pi}{\ln(R_2/R_1)} \mu C_{ox} (V_{G2} - V_{TH2/FB2}) V_D$$

S. Cristoloveanu and S. Williams, IEEE Electron Device Letters, Vol. 31, p. 102, 1992
 S. Cristoloveanu and S.S. Li, Electrical Characterization of Silicon-On-Insulator Materials and Devices, Kluwer Academic Publishers, p. 104, 1995
 D. Munteanu, S. Cristoloveanu, and H. Hovel, Electrochemical and Solid-State Letters, Vol. 2, p. 242, 1999.

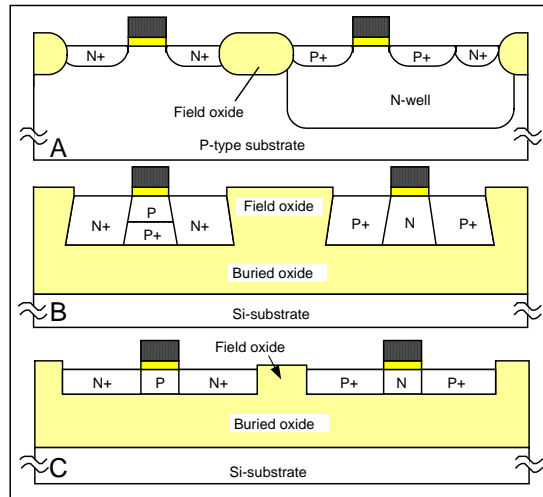
Ψ-MOSFET



I-V_G characteristics of a Ψ-MOSFET. A: fully depleted film; B: partially depleted film

S. Cristoloveanu and S. Williams, IEEE Electron Device Letters, Vol. 31, p. 102, 1992
 S. Cristoloveanu and S.S. Li, Electrical Characterization of Silicon-On-Insulator Materials and Devices, Kluwer Academic Publishers, p. 104, 1995
 D. Munteanu, S. Cristoloveanu, and H. Hovel, Electrochemical and Solid-State Letters, Vol. 2, p. 242, 1999.

CMOS Processing

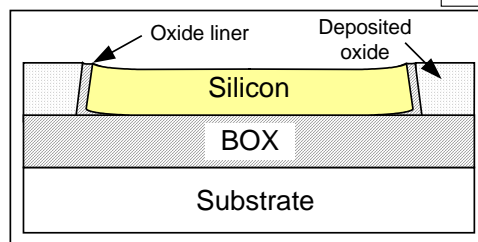
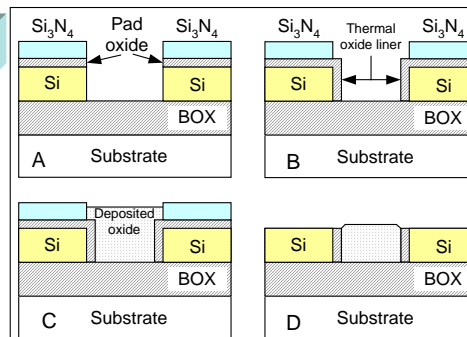


Cross-section of
 A: bulk CMOS inverter
 B: partially depleted SOI CMOS inverter, and
 C: fully depleted SOI CMOS inverter

35

Shallow Trench Isolation (STI)

Shallow trench isolation; A: lithography and nitride/pad oxide/silicon etch; B: growth of sidewall thermal oxide, C: CVD oxide deposition and CMP; D: nitride and pad oxide strip.

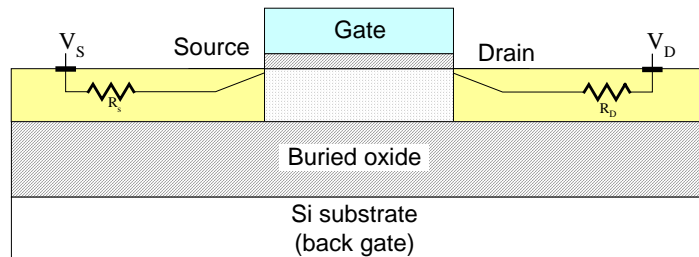


Silicon island bending caused by oxide liner growth → lower surface mobility for electrons

H. Shang, M.H. White, D.A. Adams, Proceedings of the IEEE International SOI Conference, p. 37, 2002

36

Source and drain resistance

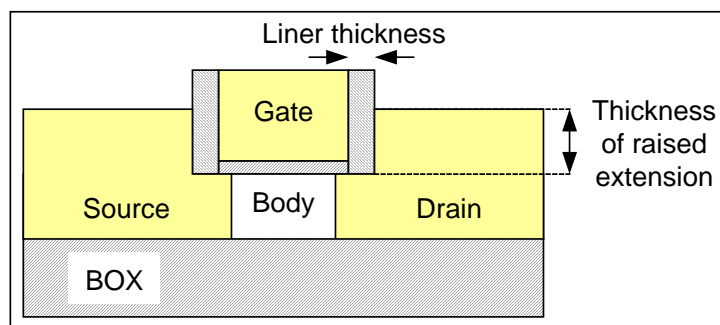


- S&D resistance become important as silicon film thickness is reduced.
- Solutions: elevated S&D
full or partial S&D silicidation
metal (Schottky) S&D

Ref: 41-43

37

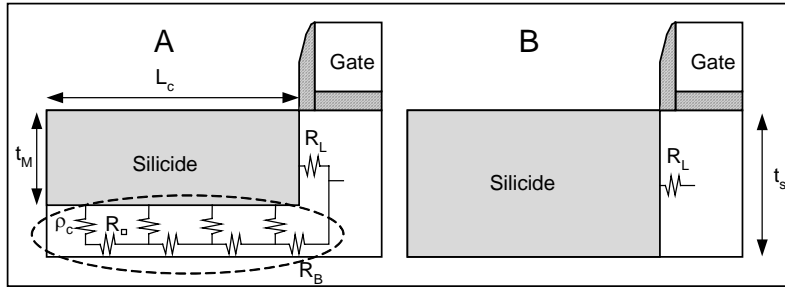
Elevated source and drain



A. Vandooren, A. Barr, L. Mathew, T.R. White, S. Egley, D. Pham, M. Zavala, S. Samavedam, J. Schaeffer, J. Conner, B.Y. Nguyen, B.E. White, Jr., M.K. Orłowski, J. Mogab, IEEE Electron Device Letters, Vol. 24, no. 5, p. 342, 2003
S.S. Kim, T.H. Choe, H.S. Rhee, G.J. Bae, K.W. Lee, N.I. Lee, K. Fujihara, H.K. Kang, J.T. Moon, Proceedings of the IEEE International SOI Conference, p. 74, 2000
J.L. Egley, A. Vandooren, B. Winstead, E. Verret, B. White, B.Y. Nguyen, Electrochemical Society Proceedings, Vol. 2003-05, p. 307, 2003

38

Silicided source and drain

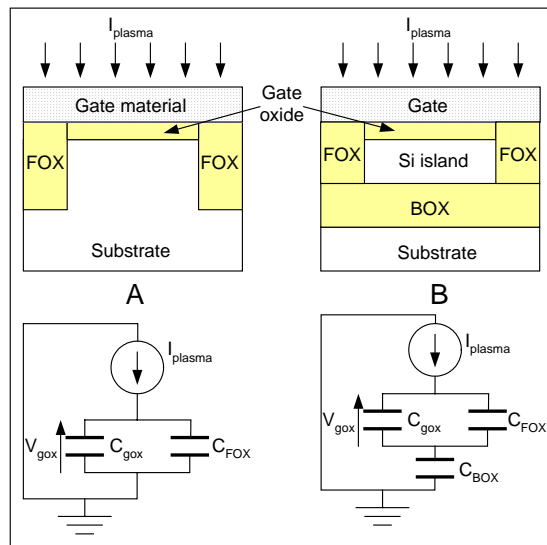


Current flow path in a silicide junction. A: the silicide is thinner than the silicon film; B: the silicide reaches the BOX

H.I. Liu, J.A. Burns, C.L. Keast, P.W. Wyatt, IEEE Transactions on Electron Devices, Vol. 45, no. 5, p. 1099, 1998
 T. Ichimori, N. Hirashita, 2000 IEEE International SOI Conference. Proceedings, p. 72, 2000
 T. Ichimori, N. Hirashita, Japanese Journal of Applied Physics Part 1, Vol. 40, no. 4B, p. 2881, 2001

39

Reduced antenna effect



Antenna effect during plasma etch step in bulk (A) and SOI (B)

A.O. Adan, T. Naka, A. Kagisawa, H. Shimizu, Proceedings of the IEEE International SOI Conference, p. 9, 1998

40

Several books have been published on SOI

